Electron and Hole Adducts Formed in Illuminated InP Colloidal Quantum Dots Studied by Electron Paramagnetic Resonance

Olga I. Mićić* and Arthur J. Nozik*
National Renewable Energy Laboratory, 1617 Cole Boulevard, Golden, Colorado 80401

Efrat Lifshitz
Solid State Institute, Technion—Israel Institute of Technology, Haifa 32000, Israel

Tijana Rajh,* Oleg G. Poluektov, and Marion C. Thurnauer*
Chemistry Department, Argonne National Laboratory, 9700 South Cass Avenue, Argonne, Illinois 60439

Received: November 14, 2001; In Final Form: February 5, 2002

An electron paramagnetic resonance (EPR) study of photoexcited colloidal InP quantum dots (QD) shows the formation of electron and hole adducts. An EPR signal at $g = 0.58$ is assigned to a nonradiative hole trap that does not form immediately upon illumination, but forms only after the illuminated sample ages and becomes stabilized at room temperature; it then becomes permanent at the InP QD surface. This signal completely disappears upon electron injection into the QD from a reducing agent (sodium biphenyl). Light immediately quenches the signal at $g = 0.58$, and it re-forms reversibly when the light is turned off. A signal at $g = 2.055$ is assigned to electron surface traps, and it appears in nonetched QD samples; it completely disappears after etching with HF. A signal at $g = 2.001$ has a very narrow line width and is assigned to delocalized mobile holes that are located in the QD core. A defect model for InP QDs is proposed based on the EPR results reported here plus results from optically detected magnetic resonance experiments reported separately.

Introduction

Semiconductor quantum dots (QDs) have been the subject of much interest over the past decade due to their remarkable physical properties and potential applications.[1−5] While the optical and electronic properties arising from quantization effects are understood to a significant degree, the effects of the surface on these properties are less well understood. However, the dependence of the photoluminescence quantum yield on surface passivation shows that surface defects play major roles in the relaxation dynamics of the electrons and the holes formed by illumination. Different types of surface defects can be produced on QD surfaces since different crystallographic planes and different In−P coordination and bond lengths are present. Also, the influence of surface states is greatly enhanced in small QDs since they have high surface-to-volume ratios (e.g., 30% of the atoms in a 35 Å diameter III−V QD are at the surface).

The uncertainty about the relative roles of the surface vs the core in determining the overall QD electronic structure stems, in part, from the lack of synthetic methods that can produce fully passivated surfaces of QDs. Also, the synthesis of colloidal InP QDs generally creates dots of different quality in the same sample. Some of them exhibit band edge emission, while others have various defect or trap states that show emission originating from trap-to-trap or trap-to-band recombination. Very recently, optically detected magnetic resonance (ODMR) studies on colloidal InP QDs show that electrons are trapped in P vacancies present both in the core and at the surface, and that they may recombine radiatively with valence band holes.[6]

To further clarify the nature of the electron and the hole traps following illumination in colloidal InP QDs, we have used electron paramagnetic resonance (EPR) techniques to study the paramagnetic species formed in nanocrystals. EPR has not been used previously to identify electron and hole adducts in semiconductor QDs; it is a powerful technique because it can detect both radiative and nonradiative paramagnetic states in the dark or in the light. In the present work, we detected a permanent paramagnetic species that can be assigned to trapped surface holes that are present in the dark in samples that have been previously illuminated. We also found other paramagnetic species that are formed in the QD core and at the surface, and we assign them to various types of electron adducts and delocalized charge.

Experimental Section

A. Synthesis of Colloidal InP QDs. Colloidal InP QDs were synthesized by colloidal chemistry methods using $InCl_3$ and tris-(trimethylsilyl)phosphine ($P(SiMe_3)_3$) as starting reactants; the reactants are heated for 3 days at 260−280 °C in the presence of trioctylphosphine oxide (TOPO) and trioctylphosphine (TOP). The synthesis was conducted in rigorously air-free and water-free atmospheres. Details of the preparation are given in refs 7 and 8. During the synthesis the QDs are capped with TOPO/TOP, which produce a compact hydrophobic shell on the particle surface. After size-selective precipitation the samples have a size distribution of about 10−13%. Intense band-edge emission from InP QDs can be achieved after etching the particles with a dilute alcoholic solution of HF.[9]

B. Characterization of the Samples. Figure 1 shows the absorption and photoluminescence (PL) spectra of unetched InP quantum dots with a diameter of about 37 Å; the PL spectra show both band-edge emission (lifetime of ∼20 ns at 295 K)[10] and trapped state emission[8] in the near-IR spectral region. This

10.1021/jp014180q CCC: $22.00
Published on Web 03/27/2002

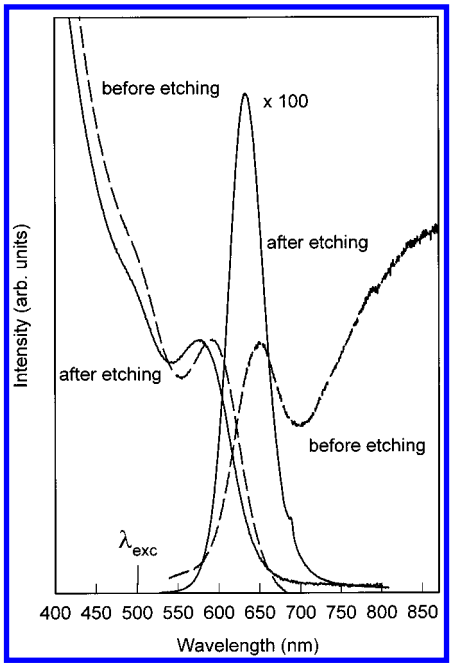

Figure 1. Absorption and emission spectra of InP QDs (diameter = 37 ± 5 Å) before and after etching.

deep trap emission arises from defect states on the QD surface, and it can be eliminated or greatly reduced by treating the QDs with HF.[9] Freshly prepared, etched QD colloidal solutions give the best emission quantum yields; over time (weeks) the QDs slowly lose emission intensity.

C. EPR Characterization. All EPR measurements were made at the Argonne National Laboratory. X-band experiments were conducted on a Bruker ESP300E spectrometer equipped with a Varian rectangular cavity TE_{102} and a variable temperature cryostat (Air Products) cooled to helium temperatures. Samples were excited either by a 300 W ILC xenon lamp with a 320-nm cutoff filter or, for higher radiant power (1−10 photons per particle), with a YAG−OPO laser (550 nm and 10−20 mJ/pulse). The samples were kept under Ar atmosphere, if not otherwise stated. Samples were excited directly in the EPR cavity at 4 K. Preliminary scans were obtained on the samples before irradiation to check for spurious signals. Temperature control for sample annealing was achieved with a Lake Shore 320 autotuning temperature controller. The sample was equilibrated for 20 min at the specified temperature before the spectrum was recorded at the temperature indicated on the figure. The g factors were calibrated by comparison to a Mn^{2+} standard in a SrO matrix ($g = 2.0012 \pm 0.0002$)[11] and with a 1,1-diphenyl-2-picrylhydrazyl (DPPH) standard ($g = 2.0036 \pm 0.0003$). A high concentration of particles (concentration of particles 10^{-5}−10^{-4} M) in 2,2,4-trimethylpentane solution and 0.05% TOPO that formed an optically clear organic glass at cryogenic temperatures was used to improve the quality of detection, as described previously.[12]

D. Optical Characterization. Steady-state photoluminescence spectra were collected at room temperature using an SPEX Model 1691 fluorolog (excitation with a xenon lamp and cooled photomultiplier tube detector). Optical absorption spectra were collected at room temperature using a Cary 5E UV−vis−near-IR spectrophotometer.

Results and Discussion

Irradiation of InP QDs with photon energy greater than the band gap leads to the generation of bound electron−hole pairs

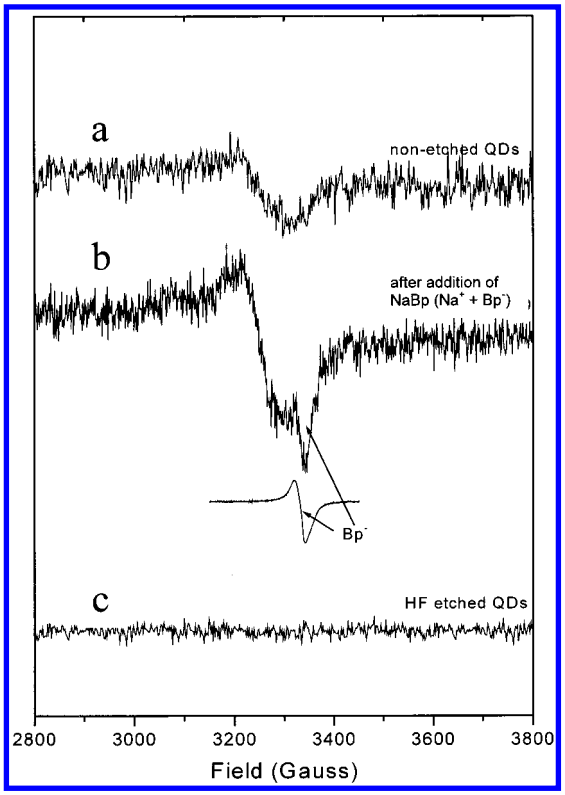

Figure 2. EPR signals of InP QDs (diameter = 47 ± 5 Å) at 4.2 K: (a) in the dark, (b) after electron injection in the dark, and (c) after HF etching and excitation with a xenon lamp. The signal at about 3350 G after electron injection (b) is due to the presence of the Bp radical. The EPR frequency is 9.345 GHz, modulation amplitude (MA) is 6.3 G, time constant is 1.28 ms, and microwave power is 2 mW.

(excitons) that can recombine to yield band edge emission, or they can ionize into separated, mobile electrons and holes that can be trapped at various defects present in the QDs. We used EPR to identify the paramagnetic species that are present in the dark and light in InP QDs; illumination was provided from two different sources of light: a xenon arc lamp and a pulsed laser (550 nm). Experiments were also carried out to distinguish the difference between intermediates that are formed with multiphoton or one-photon absorption, shown in Figures 3, 4, and 5, respectively.

A. Electron Adducts Initially Present in the Dark. The presence of structural defects such as donor or acceptor impurities, or surface states in semiconductors, is often manifested by the presence of unpaired electrons that may lead to the observation of dark EPR signals. The EPR signal of InP QDs before illumination is shown in Figure 2; a permanent species with a broad and very weak EPR signal at $g = 2.055$ and a line width of 100 G was found. To identify the nature of this signal, we injected electrons into InP QDs from sodium biphenyl (NaBp), which is a very strong reducing agent ($E_O = -2.6$ V vs NHE)[13] (see Figure 2). NaBp has previously been used to inject electrons into semiconductor QDs.[13] After injection of electrons, the intensity of the signal with $g = 2.055$ is increased. This indicates that the paramagnetic species with $g = 2.055$ is an electron adduct. The signal near $g = 2.004$ in the dark after addition of NaBp (sodium biphenyl) in Figure 2b is due to the Bp^- radical[14] that is also present in the sample.

The EPR signal obtained in the dark at $g = 2.055$ can be completely removed after the sample is etched with HF, indicating that this paramagnetic species is located at the surface. The signal at $g = 2.055$ is also the same as that obtained in illuminated InP QDs (Figure 3) upon multiphoton absorption.

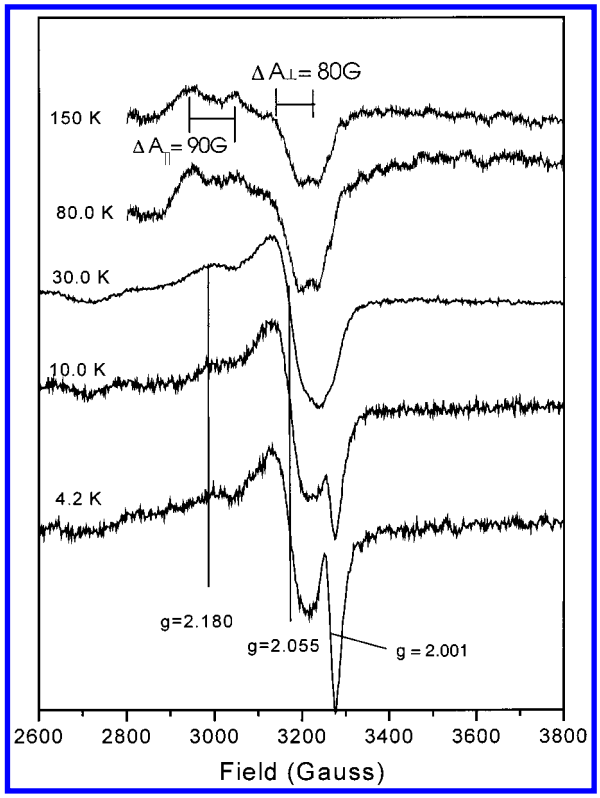

Figure 3. EPR signals of nonetched InP QDs (diameter = 40 ± 4 Å) with laser excitation (λ = 550 nm), annealed at different temperatures, and then recorded at 4.2 K. The EPR frequency (9.135 GHz) is different compared to Figure 2, but the g values of the signals are the same (8.23 G MA, 0.64 ms time constant, and 5 mW microwave power).

The line width of this signal in Figure 2 is significantly smaller than the signal of phosphorus vacancies previously observed in InP single crystals,[15] indicating that this species does not have spin density on In atoms with large spin multiplicity (9/2) and hyperfine coupling. Also, the g value of this signal indicates that the species is not centered on phosphorus atoms that display small g anisotropy. This species is different from that produced by electrons trapped at surface P vacancies that have $g = 1.93$, and a line width of 750−1000 G, as found previously by ODMR in our InP QD samples.[6] The signal at $g = 2.055$ (line width 100 G) is also different from the signal associated with the interior phosphorus vacancy with $g = 1.98$ and line width 1800 G found by ODMR for our colloidal InP QDs. EPR cannot detect the signal of P vacancies because of the lower sensitivity of the EPR technique ($>10^{14}$ paramagnetic species/cm^3) compared to ODMR ($>10^9$ species/cm^3).

B. Transients Formed in Multiphoton Absorption. When the samples were illuminated with the 550 nm laser light, with the number of photons exceeding the number of QD particles (Figure 3) in nonetched samples, two paramagnetic species were observed: the first signal, with g value the same as the dark signal at $g = 2.055$ (line width ∼100 G), and the second, with $g = 2.001$ and significantly reduced line width (line width <10 G). The intensity of the signal at $g = 2.055$ increases significantly compared to the dark signal and becomes dominant (Figure 3). The signal at $g = 2.001$ narrows as the modulation amplitude (H_m) is decreased from 6 to 1.9 G, reaching the line width of ∼2 G for H_m of 1.9 G. The optimal setting of H_m was not reached in these measurements, but the sensitivity could not be further sacrificed in order to preserve the true line shape.

In multiphoton absorption at least two electron−hole pairs will be formed simultaneously in the same QD, and Auger photoionization can occur. Annihilation of one-electron pair via an Auger process can result in a transfer of energy to a remaining carrier, most likely an electron, which can then be ejected from the nanocrystals into the surrounding matrix. The electrons can become trapped at surface defects leading to an increase of the concentration of species with $g = 2.055$. In this case the signal at $g = 2.001$ (Figure 3) can be assigned to mobile holes located in the QDs since the electrons are trapped at the surface. The large g anisotropy of the signal at $g = 2.055$ suggests that the electron is centered on the oxygen atoms that form the surface layer of nonetched samples. The relatively small width of the signal (100 G) suggests that electrons are trapped on oxygen atoms bound to phosphorus atoms having spin multiplicity of 1/2 and a hyperfine coupling constant of tens of gauss, rather than a few hundred gauss, as expected for neighboring In atoms. Additionally, spectra of annealed samples at temperatures >80 K (Figure 3) show resolved hyperfine splitting with of a nucleus with spin 1/2 centered around $g = 2.180$ and $g = 2.055$. The line shape of the spectrum is characteristic for an anisotropic hyperfine splitting of an anisotropic axially symmetric g tensor. The other possibility is that there are two P neighbors at the surface, with different distances with respect to electron spin that leads to two different nonrelated signals.[16]

The effect of temperature on the $g = 2.055$ and the 2.001 signals is completely different. The signal with $g = 2.001$ disappears at 8 K, while the signal at $g = 2.055$ slowly decreases and could be detected even after annealing to room temperature. This temperature dependence indicates that the electron adduct with $g = 2.055$ is in a deep trap, while the holes with $g = 2.001$ are in shallow trapping sites or are delocalized.

In HF-etched QDs, the surface defects are passivated by filling P vacancies with F^- ions and removing surface oxide layers. It has been shown previously that HF successfully passivated InP QDs[9] and that the passivated QDs show strong band edge emission (Figure 1). With HF etching, only the very narrow signal at $g = 2.001$ prevails (Figure 4); the intensity of the signal with $g = 2.055$ is completely suppressed, indicating that this paramagnetic species is located on the surface and is completely removed with HF treatment, while the signal at $g = 2.001$ is associated with the QD core. The intensity of the signal at $g = 2.001$ significantly increases, suggesting that upon removal of electron trapping sites from the particle surface photogenerated holes have longer lifetimes and consequently build larger steady state concentrations. In HF-etched samples, electrons most likely disappear in a reaction with impurities that are present in the surrounding solvent matrix. Figure 4 shows how this signal changes with microwave power and disappears with an increase in the annealing temperature. The shape of the line is Lorentzian (homogeneously broadened). In the solid state the Lorentzian shape is due to the high mobility of unpaired electrons (no saturation) and usually indicates that T_2 equals T_1. The width of the line is due only to the spin−lattice relaxation time ($T_1 = h/\pi g\beta\Delta H_{T_1}$) and can be obtained from the measured line width ($\Delta H = \Delta H_0 + \Delta H_{T_1}$).[17] At elevated temperatures (t), the signal slightly broadened in agreement with a shortened spin−lattice relaxation[18,19] (Figure 4a insert) and was found to vary as $t^{5/2}$ attributed to the spin−orbit coupling with lattice vibrations.[20] The relaxation time determined from the line width at 4.2 K (1.14 G, H_m 0.2 G) is 100 ns, while it shortens to 60 ns at 180 K. This relaxation process is fast enough that the signal does not saturate at microwave powers as high as 5 mW. Saturation properties of this species are shown in the insert in Figure 4b. There is no change of the line width with an increase of the power (P), and the signal intensity was found to be proportional

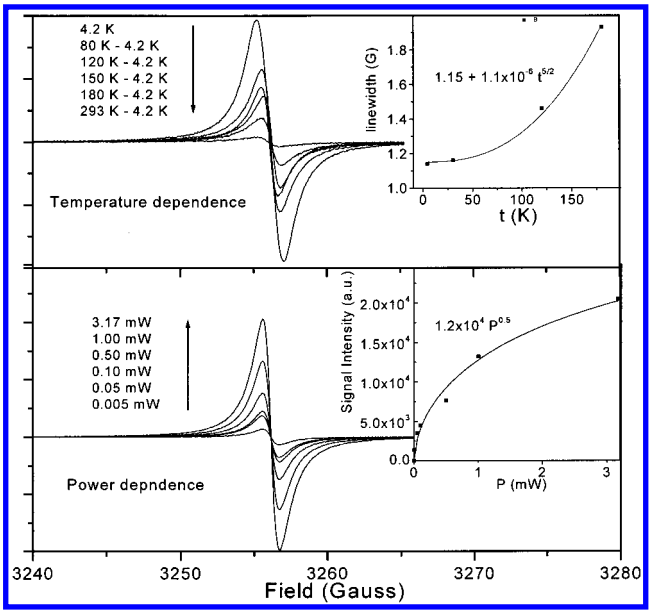

Figure 4. EPR signals of HF-etched InP QDs (diameter = 44 ± 4 Å) excited with a laser (λ = 550 nm): (a) the sample is annealed at different temperatures and recorded at 4.2 K (the insert shows line broadening versus recorded temperature and the fitted line corresponding to the indicated function); (b) EPR spectra obtained at different microwave output powers (0.005, 0.05, 0.1, 0.5, 1.0, and 3.17 mW) (the insert shows the power dependence of the signal amplitude and the fitted line corresponding to the indicated function). The EPR frequency is 9.121 GHz, MA is 0.199 G, time constant is 0.54 ms, and microwave power is 0.005 mW.

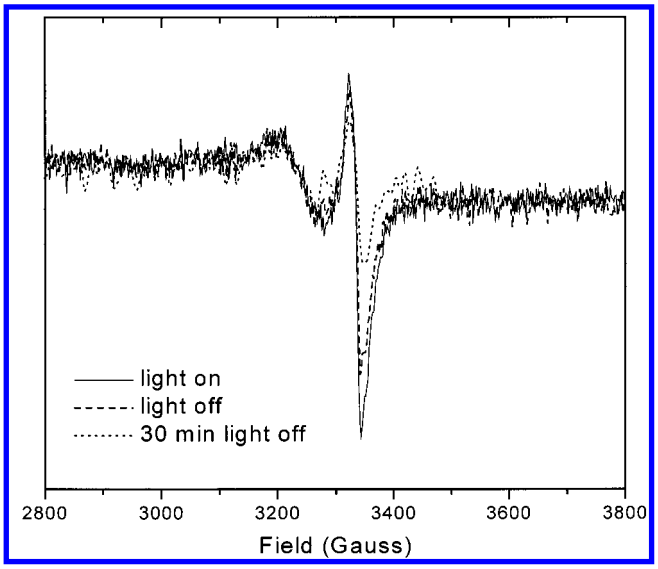

Figure 5. Light-induced EPR signals during a light-on period and after the light is turned off. The spectra of InP QDs (diameter 47 ± 5 Å) were recorded at 4.2 K and excitation is with a xenon lamp. The EPR frequency is 9.345 GHz, MA is 6.3 G, time constant is 1.28 ms, and microwave power is 2 mW.

to $P^{1/2}$ (Figure 4b, insert). There is no broadening of the resonance with an increase in the light intensity previously observed in highly doped III−V semiconductors and attributed to spin−spin interaction.[21] The Lorentzian shape and small line width of the signal also suggest that the radical species giving rise to this resonance is highly delocalized and does not feel the lattice environment. This suggests that delocalized radical species, most probably delocalized holes, exhibit resonance at $g = 2.001$.

C. Paramagnetic Electron and Hole Species Formed by Low Light Intensity. When nonetched samples were illuminated with the xenon lamp (Figure 5) with light intensity having ≪1 photon per particle, both paramagnetic species that exhibit EPR signals at $g = 2.055$ and $g = 2.001$ were observed. The signal at $g = 2.055$, which is present in the dark before illumination, increases only slightly upon illumination with low-intensity light. The signal at $g = 2.001$ is only formed by light and slowly disappears after the light is turned off (Figure 5). It does not convert in the dark into the signal with $g = 2.055$, confirming its nature as photogenerated holes. The signal at $g = 2.001$ has the same saturation properties as the signal at $g = 2.001$ obtained with high-intensity light (Figure 4). The narrow line width (1 G) suggests that this species does not feel the presence of the In atoms, which have a nuclear spin of 9/2 and a large coupling constant of 350 G. This means that this paramagnetic species is insensitive to the environment and therefore delocalized; it is also insensitive to P atoms as well, as P atoms have a nuclear spin of 1/2 that should appear in the spectra as a set of doublets with significant hyperfine couplings. In bulk InP, the conduction band electrons have a very narrow signal with $g = 1.20-1.50$.[22−24] It is expected that the g value increases with decreasing particle size because of the different QD boundary conditions,[25,26] and it can be larger than that for bulk InP. The valence band holes of bulk InP have an EPR signal at $g = 0.97$,[27] and this is also far from the signal we observe at $g = 2.001$. The fact that the signal disappears relatively slowly with time (Figure 5) at 4.2 K suggests that the species is capable of diffusing at this temperature, and that this paramagnetic species is not deeply trapped, but rather is in shallow traps or is a mobile delocalized species. Electrons and holes cannot coexist in the QD core for 30 min since they undergo recombination or the more mobile electron is trapped at the surface relatively quickly. From these results we conclude that the signal at $g = 2.001$ arises from delocalized holes in the QD core.

The EPR signal for bound electron−hole pairs (excitons) that form in QDs during the absorption of light cannot be seen because EPR can only detect paramagnetic species that reach a steady-state concentration of $\sim 4 \times 10^{12}$ spins per cm^3 at 10 K for a 20 G wide signal. In QDs, the excitons are dissociated by trapping of electrons and/or holes into energetically favorable defect states.[28,29]

D. Origin of Permanently Trapped Holes. After exposure of InP QDs to light, an EPR signal with $g = 0.58$ and line width of 50 G develops. The mechanism of formation of this species is quite complex. Before exposure to light and during illumination at 4 K, this signal could not be observed. However, after the sample is warmed to room temperature, aged, and cooled to 4 K, a strong signal at $g = 0.58$ appears in the dark (Figure 6a). Perhaps this species is stabilized by slow structural rearrangement at room temperature. This signal has an asymmetric Dysonian shape, and this suggests that the holes have some degree of mobility. This could possibly arise from a hopping mechanism between hole trap sites inside the same QD. In that case, the signal represents a sum of individual symmetric spectra of charge carriers having different center field positions because each charge carrier feels a magnetic field with a different amplitude and phase, resulting in distortion of signal shape. There is also a possibility that the asymmetric shape is the result of axial anisotropy.

The signal at $g = 0.58$ does not exist in samples that are freshly prepared. Also, this signal completely disappears after injection of electrons from NaBp (Figure 6b), indicating that this species is a hole adduct and does not recover immediately

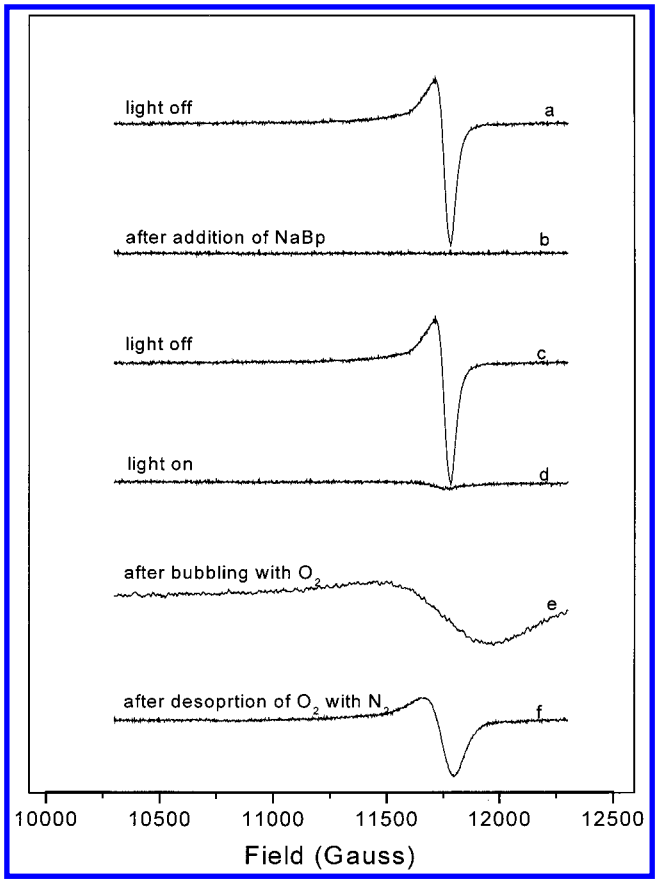

Figure 6. EPR signal of InP QDs (diameter 47 ± 5 Å) of light-induced hole traps at $g = 0.58$ in the dark (a, c) and the effects of (b) electron injection, (d) illumination, (e) exposure to oxygen, and (f) removal of oxygen. The temperature was 4.2 K, and the sample was excited with a xenon lamp. The EPR frequency is 9.346 GHz, MA is 6.3 G, time constant is 1.28 ms, and microwave power is 2 mW.

during illumination. NaBp also quenches the PL emission, and when NaBp is removed from solution, the emission is reestablished while PL upconversion (see section E below) completely disappears.

The paramagnetic species with $g = 0.58$ has the same characteristics as the positive charge observed directly in CdSe with electrostatic force microscopy by Brus et al.[30] They found that electrostatic polarization among individual QDs is nonuniform and that about half of the QDs present in a CdSe sample possess a positive charge that is created by low light intensity and after aging.[31]

The species with signal at $g = 0.58$ exhibits additional complicated behavior. The signal disappears with illumination (Figure 6d) and re-forms reversibly when the light is turned off (Figure 6c). The effect of the presence of oxygen on the nature of the species with $g = 0.58$ is shown in Figure 6e. Adsorption of oxygen to the QD surface affects the hole trapping sites, changing the shape and the line width of the EPR signal (480 G); this modification of the trap states reversibly recovers back to its initial paramagnetic species in a nitrogen atmosphere (Figure 6f). Strong response to the presence of adsorbed oxygen shows that the EPR signal with $g = 0.58$ is a hole adduct trapped on the particle surface.

Thus, these experiments show that two permanent nonemissive trapping states are formed on the InP QD surface upon photoexcitation: an electron trapping site with $g = 2.055$ (formed under illumination in freshly prepared QDs) and a hole trapping site with $g = 0.58$ (formed after illumination in aged samples). However, these defects may not be present in all QDs

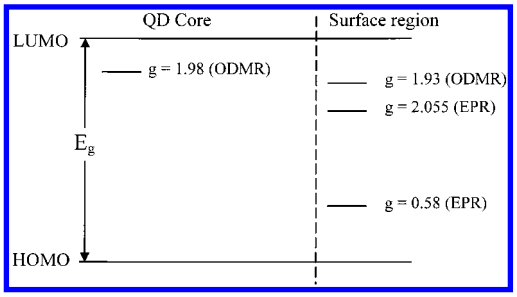

Figure 7. Schematic model of the energy states and g factors of defect/trap centers in InP QDs at the core and at the surface.

in the colloidal QD sample; during synthesis some QDs form without defect sites and show band edge or deep trapped radiative emission. When present, both of these surface defects can be passivated with HF and NaBp. EPR results can be used as a guide for the preparation of colloidal QD ensembles with better quality.

E. Defect Centers in InP QDs. The EPR results reported here, together with the ODMR results reported elsewhere on the same InP QDs,[6] lead to a proposed model for the defect structure of InP QDs, presented schematically in Figure 7. Although this model is more complicated than the one initially proposed to explain PL upconversion in QDs,[32] it is still consistent with the proposed upconversion mechanism.

The defect model (Figure 7) shows the energy levels (and g factors) of two regions associated with the core and the surface of the QD. In the core, a deep radiative electron trap that is associated with a phosphorus vacancy ($g = 1.98$) has been identified in ODMR experiments; the depth of this trap is estimated to be about 0.3 eV below the conduction band. ODMR results also indicate the presence of a deep radiative electron trap (about 0.4 eV) at the surface ($g = 1.93$). In unetched samples, the surface electron trap dominates. The EPR results indicate the presence of a nonradiative (permanent) hole trap at the surface ($g = 0.58$), plus a second, nonradiative surface electron trap at $g = 2.055$. This surface electron trap is not the same as that produced by a phosphorus vacancy; furthermore, the observation that this surface trap exists in the dark indicates that it is deep and below the Fermi level of the QD. The EPR results also show mobile, delocalized species at $g = 2.001$ which is assigned to a mobile hole in the QD core.

The model in Figure 7 shows bulk and surface state energy levels that are consistent with the calculations of Fu and Zunger.[33] The P vacancies and their energy levels and total momentums in the core ($g = 1.98$) and at the surface ($g = 1.93$) are in agreement. There is also agreement with the existence of a deep hole trap at the surface (attributed to a P dangling bond by Fu and Zunger).

Concerning PL upconversion, the proposed mechanism involves an initial optical transition from the empty hole traps (filled with electrons) at the surface to either the empty electron traps or to the conduction band (LUMO) state; the former obtains at small QD diameters while the latter obtains at large QD diameters.[33] The next step is a promotion of the trapped hole to the valence band state (HOMO) by phonon absorption, followed by upconverted PL emission from electrons in the radiative electron traps or LUMO states to HOMO states. The hole trap is identified with the $g = 0.58$ hole state in Figure 7. This is based on the fact that when this state is absent (for example, in freshly prepared InP QD colloids that have not been exposed to light), then the $g = 0.58$ line is absent from the EPR spectrum and PL upconversion also cannot be observed.

We also found that injected electrons from NaBp will quench both upconversion and the signal at $g = 0.58$.

Conclusion

Using EPR, combined with previous ODMR studies, we have established in detail the defect structure of InP QDs both in the core of the QD and at its surface. EPR results show that in freshly prepared and unetched InP QDs an electron trap is formed at the surface with $g = 2.055$. The EPR signal associated with this surface trap can be removed by etching and passivating the QDs with HF; this signal is present in the dark and also upon photoexcitation with either a laser (550 nm) or a xenon lamp. Photoexcitation at 4 K followed by warming to room temperature, aging, and recooling to 4 K results in the formation of a permanent hole trap at the surface with $g = 0.58$. This implies that the permanent hole trap, creating a permanent positive surface charge, develops from a structural rearrangement of the surface of freshly prepared QDs after photoexcitation and aging at room temperature. Under photoexcitation, a narrow EPR signal at $g = 2.001$ also forms; this signal is assigned to mobile, delocalized holes in the core of the QD. The complementary ODMR results on these InP QDs also indicate the presence of radiative electron traps created by phosphorus vacancies both at the surface (with $g = 1.930$) and in the QD core (with $g = 1.98$). The surface P vacancies can be removed by etching with HF. The EPR results show that the excitons initially created in the QDs upon absorption of light are rapidly dissociated by electron trapping into the surface defects, leaving behind free, delocalized holes in the QD core. With aging at room temperature, these holes ultimately become trapped into surface defects producing a permanent positive surface charge. The degree of surface passivation and aging time controls the presence of electron and holes at the various QD surface traps and their respective histories; this also affects the quantum yield of radiative emission from the QDs as well as PL upconversion.

Acknowledgment. The work at Argonne National Laboratory and NREL was supported by the U.S. Department of Energy, Office of Science, Office of Basic Energy Sciences, Division of Chemical Sciences, Geosciences, and Biosciences. E.L. was supported by the U.S.−Israel Binational Science Foundation.

References and Notes

(1) Brus, L. *Appl. Phys. A* **1991**, *53*, 465.
(2) Alivisatos, A. P. *Science* **1996**, *271*, 933.
(3) Bawendi, M. G. *NATO ASI Ser. B* **1995**, 339.
(4) *Science and Engineering of One- and Zero-Dimensional Semiconductors*; Beaumont, S. P., Sotomayor Torres, C. M., Eds.; Plenum Press: New York, 1990; Vol. 214.
(5) Yoffe, A. D. *Adv. Phys.* **1993**, *42*, 173.
(6) Langof, L.; Ehrenfreund, E.; Lifshitz, E.; Mićić, O. I.; Nozik, A. J. *J. Phys. Chem. B* **2002**, *106*, 1606.
(7) Mićić, O. I.; Curtis, C. J.; Jones, K. M.; Sprague, J. R.; Nozik, A. J. *J. Phys. Chem.* **1994**, *98*, 4966.
(8) Mićić, O. I.; Sprague, J. R.; Curtis, C. J.; Jones, K. M.; Machol, J. L.; Nozik, A. J.; Giessen, H.; Fluegel, B.; Mohs, G.; Peyghambarian, N. *J. Phys. Chem.* **1995**, *99*, 7754.
(9) Mićić, O. I.; Sprague, J. R.; Lu, Z.; Nozik, A. J. *Appl. Phys. Lett.* **1996**, *68*, 3150.
(10) Mićić, O. I.; Cheong, H. M.; Fu, H.; Zunger, A.; Sprague, J. R.; Mascarenhas, A.; Nozik, A. J. *J. Phys. Chem. B* **1997**, *101*, 4904.
(11) Rosenthal, J.; Yarmus, L. *Rev. Sci. Instrum.* **1966**, *37*, 381.
(12) Rajh, T.; Ostafin, A. E.; Mićić, O. I.; Tiede, D. M.; Thurnauer, M. C. *J. Phys. Chem.* **1996**, *100*, 4538.
(13) Shim, M.; Guyot-Sionnest, P. *Nature* **2000**, *407*, 981.
(14) Gribnau, M. C. M.; De Boer, E. *Mol. Phys.* **1991**, *73*, 819.
(15) Von Berdeleben, H. J. *Solid State Commun.* **1986**, *57*, 137.
(16) Sibley, S. P.; Francis, A. H.; Lifshitz, E. *J. Phys. Chem.* **1994**, *98*, 5089.
(17) Standley, K. J.; Vaughan, R. A. *Electron Spin Relaxation Phenomena in Solids*; Adam Hilger, Ltd.: London, 1969.
(18) Lancaster, G.; van Wyk, J. A.; Schneider, E. E. *Proc. Phys. Soc.* **1964**, *84*, 19.
(19) Poris, A. M.; Kip, A. F.; Kittel, C.; Brattain, W. H. *Phys. Rev.* **1953**, *90*, 488.
(20) Yafet, Y. *Solid State Physics*; Academic Press: New York, 1963; Vol. 14.
(21) Bemski, G. *Phys. Rev. Lett.* **1960**, *4*, 62.
(22) Chen, Y.; Gil, B.; Mathieu, H.; Lascaray, J. P. *Phys. Rev. B* **1987**, *36*, 1510.
(23) Clerjaud, B.; Gendron, F.; Obloh, H.; Schneider, J.; Wilkening, W. *Phys. Rev. B* **1989**, *40*, 2042.
(24) Dawei, Y.; Cavenett, B. C.; Skolnick, M. S. *J. Phys. C.: Solid State Phys.* **1983**, *16*, L647.
(25) Rodina, A. V.; Efros, A. L.; Rosen, M.; Meyer, B. K. Unpublished results.
(26) Gupta, J. A.; Awschalom, D. D.; Peng, X.; Alivisatos, A. P. *Phys. Rev. B* **1999**, *59*, R10 421.
(27) Bimberg, D.; Hess, K.; Liparri, N. O.; Fishbach, J. U.; Alferelli, M. *Physica B* **1977**, *89*, 139.
(28) Sercel, P. C. *Phys. Rev. B* **1995**, *51*, 14532.
(29) Bawendi, M. G.; Wilson, W. L.; Rothberg, L.; Carroll, P. J.; Jedju, T. M.; Steigerwald, M. L.; Brus, L. E. *Phys. Rev. Lett.* **1990**, *65*, 1623.
(30) Krauss, T. D.; Brus, L. E. *Phys. Rev. Lett.* **1999**, *83*, 4840.
(31) Krauss, T. D.; O'Brien, S.; Brus, L. E. *J. Phys. Chem. B* **2001**, *105*, 1725.
(32) Poles, E.; Selmarten, D. C.; Mićić, O. I.; Nozik, A. J. *Appl. Phys. Lett.* **1999**, *75*, 971.
(33) Fu, H.; Zunger, A. *Phys. Rev. B* **1997**, *56*, 1496.